Arch. Metall. Mater. **64** (2019), 1, 39-43

DOI: 10.24425/amm.2019.126216

V. VIGNAL*#, H. KRAWIEC**, M. LATKIEWICZ**

INFLUENCE OF DISSOLVED OXYGEN ON THE CORROSION BEHAVIOUR IN RINGER'S SOLUTION AND ARTIFICIAL SALIVA OF Co-Mo NANO-CRYSTALLINE COATINGS ELECTRODEPOSITED ON Co AND 316L SUBSTRATES

The influence on the corrosion behaviour of Co-Mo nano-crystalline coatings of dissolved oxygen is studied in the Ringer's solution and artificial saliva at 25°C. This was done by means of potentiodynamic tests and surface observations. It was shown that dissolved oxygen has no influence on passivity, oxidation of the coating and selective dissolution of cobalt. By contrast, dissolved oxygen affects corrosion. General corrosion was observed in the Ringer's solution whereas pitting corrosion was found in artificial saliva.

Keywords: cobalt, molybdenum, nano-crystalline coating, corrosion, dissolved oxygen

1. Introduction

Numerous papers [1-6] have shown that nano-crystalline coatings electrodeposited on metallic substrates have good physical-chemical properties. They are characterized by high hardness and high thermal resistance. In addition Co-Mo coatings have good magnetic properties and they are good catalytic electrodes for hydrogen evolution reaction. Therefore, Co-Mo nano-crystalline coatings are promising materials in various industrial sectors: biology, energy, nanotechnologies, aerospace [7].

Only a few papers [8-11] have been devoted to the corrosion behaviour of Co-Mo nano-crystalline coatings. Corrosion tests were performed in acidic (6M HCl [8]) and neutral (7 g/L Na_2SO_4 + 7 g/L NaCl [9] and 0.5M NaCl [10]) solutions. All these investigations have shown that Co-Mo nano-crystalline coatings exhibit complex corrosion behaviour. Their structure and chemical composition are important parameters in understanding corrosion mechanisms. Recently, corrosion mechanisms in the Ringer's solution (aerated solution) have been identified from potentiodynamic tests, surface observations and chemical analysis [11]. The following regions were found in the anodic branch of polarisation curves with increasing applied potential: passivity (region I), oxidation of the coating (region II), selective dissolution of Co (region III) and corrosion (region IV).

In the present paper, the influence on the corrosion behaviour of Co-Mo nano-crystalline coatings (existence of the different regions) of dissolved oxygen is studied in the Ringer's solution and in artificial saliva. This was done by means of potentiodynamic tests and surface observations.

2. Materials, and methods

2.1. Materials and surface preparation

Co-Mo nano-crystalline coatings were electrodeposited on ultra-pure Co (chemical composition (wt.%): 99.999+% Co, Al < 1 ppm, Ag < 2 ppm, Cr < 1 ppm, Cu < 3 ppm, Fe < 7 ppm, Mg < 1 ppm and Si < 5 ppm) and on type 316L stainless steel (SS) (chemical composition (wt.%) : 0.019% C, 0.41% Si, 1.57% Mn, 0.031% P, 0.029% S, 16.95% Cr, 2.03% Mo, 11.05% Ni, 0.4% Cu, 0.2% Co and 0.035% N, bal. is Fe). The two substrates were delivered by Goodfellow. They were first mechanically ground with emery papers (down to 4000 grit), cleaned in ethanol under ultrasonics for 5 min and then dried in air.

Co-Mo nano-crystalline coatings were electrodeposited in 0.2M $CoSO_4$ $7H_2O$ + 0.02M Na_2MoO_4 $2H_2O$ + 0.5M H_3BO_3 + 0.3M $Na_3C_6H_5O_7$ (pH = 5.8, temperature = 25°C, 260 rpm). Electrodeposition was carried out under potentiostatic condition (–1.2 V vs. SCE) for 5 min. These conditions were defined in a preliminary study [11]. Under these conditions (5 minutes of electrodeposition), the thickness coating does not exceed 2 µm. The counter and reference electrodes were a Pt foil and a saturated calomel reference (SCE), respectively.

2.2. Corrosion tests and surface observations

Corrosion tests were carried out in the Ringer's solution (8.6 g/L NaCl, 0.3 g/L KCl and 0.48 g/L $CaCl_2$) and in artificial

* ICB UMR 6303 CNRS - UNIVERSITÉ BOURGOGNE FRANCHE-COMTÉ, DIJON, FRANCE
** AGH-UNIVERSITY OF SCIENCE AND TECHNOLOGY, FACULTY OF FOUNDRY ENGINEERING, REYMONTA 23 STR., 30-059 KRAKOW, POLAND
# Corresponding author: vincent.vignal@u-bourgogne.fr

saliva (0.7 g/L NaCl, 1.2 g/L KCl, 0.2 g/L $KH_2PO_4.2H_2O$, 1.5 g/L $NaHCO_3$, 0.26 g/L NaH_2PO_4, 0.33 g/L KSCN) at 25°C. The pH of both solutions was adjusted to 7.2 (by adding NaOH). An AUTOLAB potentiostat/ galvanostat and a classical three-electrode cell were used. Polarisation curves (1 mV/s) were plotted from -850 mV vs. Ag/AgCl up to ~300 mV vs. Ag/AgCl. No prior polarisation in the cathodic domain was performed. As soon as the corrosion tests were stopped, samples were cleaned in distilled water under ultrasonics for 5 minutes. The specimen surface was then observed by means of optical microscopy (Nikon, Eclipse LV150).

3. Results and discussion

The structure of the Co-Mo nano-crystalline coating electrodeposited on Co was previously studied by means of field emission scanning electron microscopy (FE-SEM) coupled with energy dispersive X-ray spectroscopy (EDS) and X-ray diffraction (XRD) [11]. These coatings consist of hard oxide particles (diameter less than 1 μm) uniformly dispersed in a Co-Mo alloy matrix, Fig. 1(a-b). Oxide particles appear in black in Fig. 1(b). Their chemical composition is (15 kV): 28.7 at.% C, 8.7 at.% O, 14.6 at.% Mo and 48 at.% Co. The crystallite size (determined by XRD) is ~2 nm. Note that the same results were found for the coating electrodeposited on 316L SS, indicating that the substrate properties have no influence on the structure / chemical composition of the coating.

3.1. Corrosion behaviour in the Ringer's solution

Fig. 2(a) shows the polarisation curves in the Ringer's solution of the Co-Mo nano-crystalline coatings electrodeposited on Co and 316L SS. These experiments were performed in aerated and de-aerated solutions. De-aeration was carried out by bubbling nitrogen through the solution for 1 hour (before potentiodynamic tests). Whatever the experimental conditions (aerated and de-aerated solutions), the coatings electrodeposited on Co and 316L SS substrates have the same electrochemical response. This result was expected as the two coatings have the same structure and chemical composition. In the cathodic domain, the main reaction is the oxygen reduction reaction (ORR, reaction 1). The current density was then lowered in the de-aerated solution, as shown in Fig. 2(a).

$$O_2 + 2H_2O + 4e^- \rightarrow 4OH^- \qquad E^0 = 0.4 \text{ V vs. NHE} \quad (1)$$

In the two solutions, a passive region was observed within roughly the same potential range (from the corrosion potential to –0.6 V vs Ag/AgCl). It is due to the existence of a native passive film formed spontaneously on the Co-Mo nano-crystalline coatings in air after surface preparation. This native passive film is stable under cathodic polarisation and dissolved oxygen does not affect significantly its physical-chemical characteristics. Indeed, it has been demonstrated [12] that dissolved oxygen is capable of polarising metals into the passive region (under free corrosion conditions), but provides no chemical species necessary for passivation. The native passive film formed on the coating electrodeposited on pure Co was previously studied by means of XPS and Auger [11]. As the coatings formed on the two substrates have the same structure and chemical composition, one may assume that the two native passive films have the same physical-chemical characteristics.

The presence of dissolved oxygen has no influence on region II. Indeed, the same current density values were measured with the two solutions in this region (Fig. 2(a)). Surface observations by optical microscopy show that the coating is intact after stopping the polarisation curve in region II (Fig. 2(b) in aerated solution). There is no corrosion damage. Enrichment in oxygen is detected in the two coatings (formed on Co and 316L substrates) by FE-SEM/EDS in region II. Therefore, oxidation of the two coatings occurs. Under polarisation control, oxidation is due to the reaction of the metal surface with water to form an oxide (reaction 2 with M = Co or Mo). Bubbling of nitrogen re-

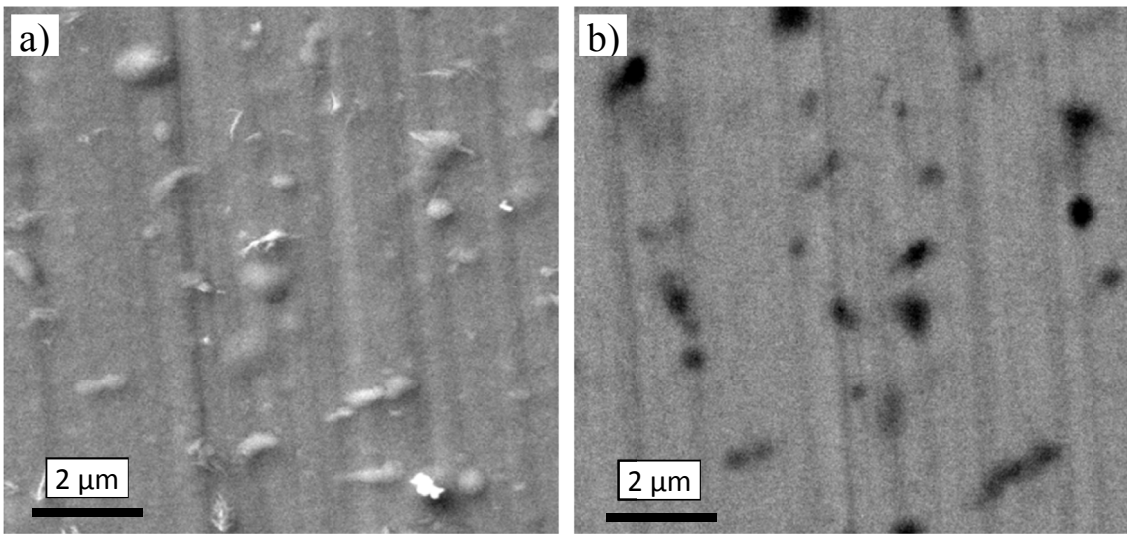

Fig. 1. FE-SEM images of the Co-Mo nanocrystalline coating electrodeposited on pure Co: (a) topological and (b) chemical modes

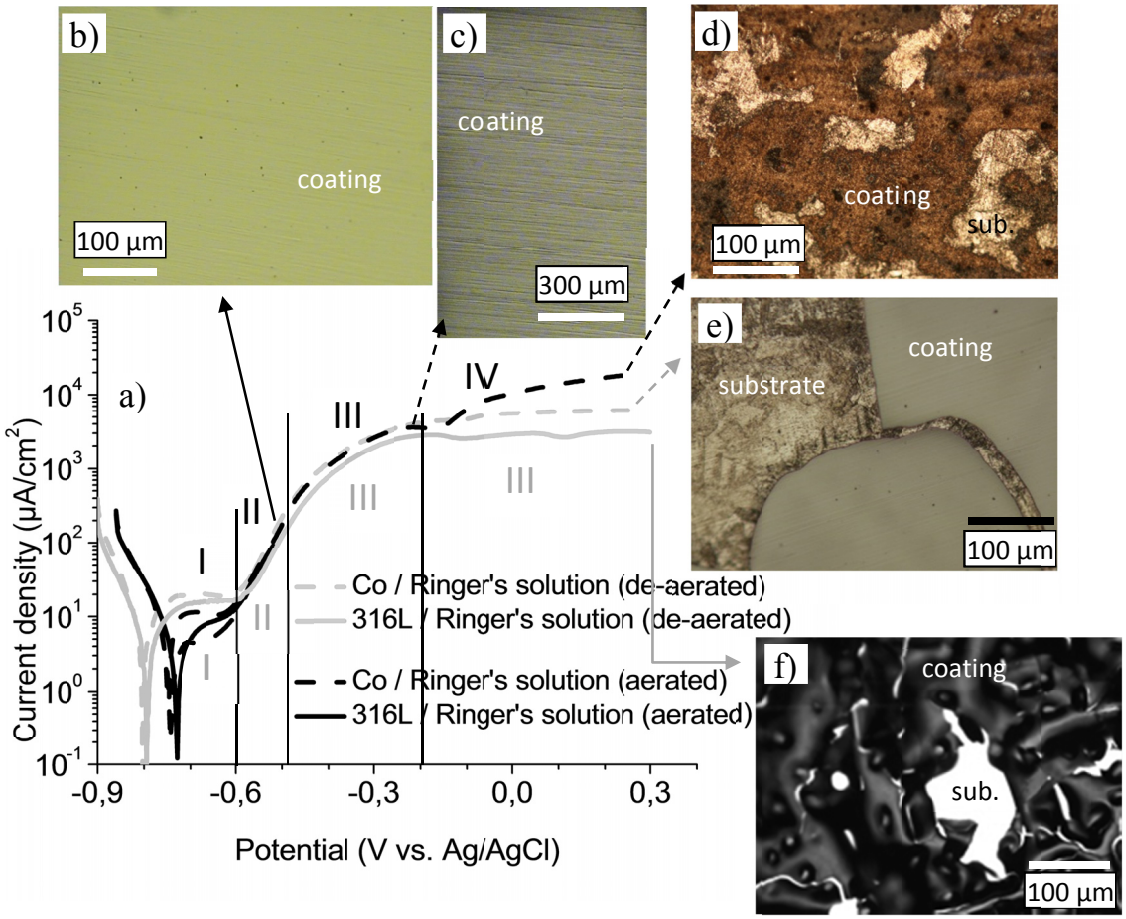

Fig. 2. Polarisation curves (1 mV/s) of the Co-Mo nanocrystalline coatings in the Ringer's solution: aerated (black curves) and de-aerated (grey curves) solutions. (b-f) Optical images of the surface after polarisation curves

duces dissolved oxygen concentration in the solution. However, bubbling does not reduce the oxidation of the coating since the coating is held under potential control (reaction 2).

$$x\,M + y\,H_2O \rightarrow M_xO_y + 2y\,H^+ + 2y\,e^- \qquad (2)$$

The presence of dissolved oxygen has also no influence on the current density value measured in region III. Depletion in Co was detected by FE-SEM/EDS in the two coatings. This means that selective dissolution of Co occurs in the two solutions (with the same kinetics). It proceeds according to reaction 3. The standard potential of Co/Co^{2+} (reaction 3) is –490 mV vs Ag/AgCl. It corresponds to the transition between regions II and III in Fig. 2(a). As it was already observed at the end of region II, the coating is intact at the end of region III and no corrosion damage is found by optical microscopy (Fig. 2(c) in aerated solution).

$$Co \rightarrow Co^{2+} + 2e^- \qquad (3)$$

By contrast, region IV exists only in the presence of dissolved oxygen, Fig. 2(a). The onset of region IV is associated with the current density increase observed from an applied potential of –200 mV vs Ag/AgCl. By contrast to regions II and III, the coating is significantly damaged. Surface observations after polarisation curves show that both spallation and corrosion occur, Fig. 2(d) in aerated solution. High levels of residual stress are generated in the coating and at the substrate / coating interface during oxidation (from region II) and selective dissolution of Co (from region III), leading to spallation. The substrate is then partly exposed to the solution (Fig. 2(d) in aerated solution). In addition, the coating which remains at the surface is rough and no pits are observed, suggesting that general corrosion takes place.

In the absence of dissolved oxygen, a current plateau is reached (no current density increase) and region III extends to very anodic potentials (no region IV). In this case, only spallation is observed, Fig. 2(e-f) in de-aerated solution. There is no corrosion and the coating which remains at the surface is intact. Corrosion of the Co-Mo nano-crystalline coating is then prevented in the absence of dissolved oxygen.

3.2. Corrosion behaviour in artificial saliva

Fig. 3(a) shows the polarisation curves in artificial saliva (aerated solution) of the Co-Mo nano-crystalline coatings electrodeposited on the two substrates. The same electrochemical response was again obtained for the two coatings. The current density in the cathodic domain was greater in artificial saliva than in the Ringer's solution, leading to a shift to the potential cor-

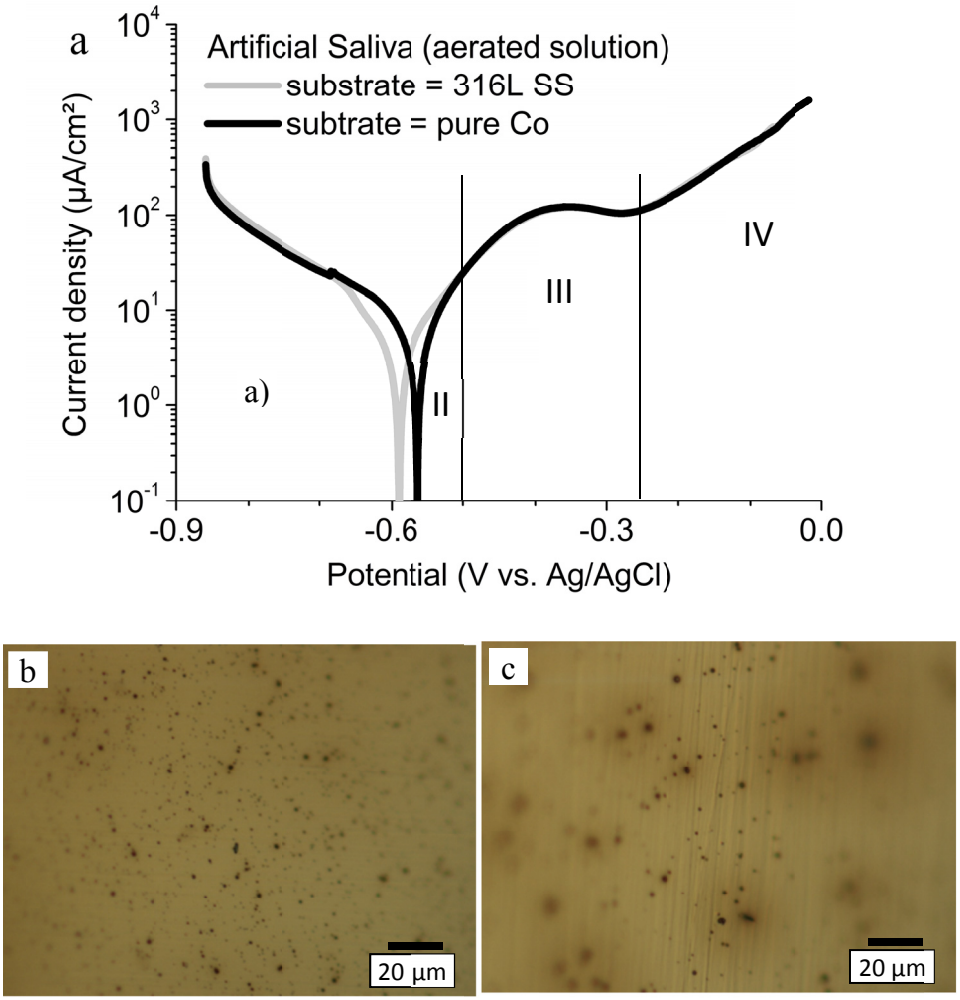

Fig. 3. (a) Polarisation curves (1 mV/s) of the Co-Mo coatings in artificial saliva (aerated solution). Optical images after polarisation curves of the Co-Mo coating electrodeposited on : (b) 316L SS, (c) Co

rosion to the anodic direction (shift of about 200 mV). Region I associated with passivity was then masked in artificial saliva.

Regions II is observed within a very narrow potential range (oxidation of the coating), Fig. 3(a). A current density plateau is again reached in region III (selective dissolution of Co according to reaction (3)). The current density in regions II and III was found to be significantly lower (and therefore kinetics of oxidation and selective dissolution of Co) than in the Ringer's solution. This may be due to the fact that the chloride content is lower in artificial saliva than in the Ringer's solution. Chloride may promote oxidation and dissolution processes. In artificial saliva, therefore, the level of internal stress in the coating and interfacial stress at the substrate/coating interface is significantly lower than in Ringer's solution. No spallation was then observed after polarisation curves (Fig. 3(b-c)).

Region IV is again associated with a current density increase (from an applied potential of –280 mV vs Ag/AgCl, Fig. 3(a)) The transition between Region III and IV is observed from an applied potential (–280 mV vs Ag/AgCl) which is less noble than that measured in the Ringer's solution (–200 mV vs Ag/AgCl). This may be due to the fact that the coating is less oxidized in artificial saliva, and therefore more reactive. Surface observations at the end of the polarisation curves (Fig. 3(b-c)), shows that numerous small pits initiated in both coatings. Similar pit morphology was observed in the two coatings, suggesting that corrosion mechanisms were identical in both cases. By contrast to what was observed in the Ringer's solution (general corrosion), localized corrosion is observed in artificial saliva.

In the de-aerated solution (Fig. 4(a)), only region III (oxidation of the coating and selective dissolution of Co) and IV (pitting corrosion) are observed. In region III, the current density remains practically constant. The density of pits in region IV (Fig. 4(b-c)) was found to be significantly lower than in the presence of dissolved oxygen. Dissolved oxygen again play a keyrole in corrosion mechanisms (as it ws observed in the Ringer's solution). The absence of dissolved oxygen prevents corrosion.

4. Conclusions

It was shown that dissolved oxygen has no influence on passivity / oxidation of the Co-Mo nano-crystalline coatings and selective dissolution of cobalt. By contrast, dissolved oxygen affects corrosion processes observed at high applied potentials.

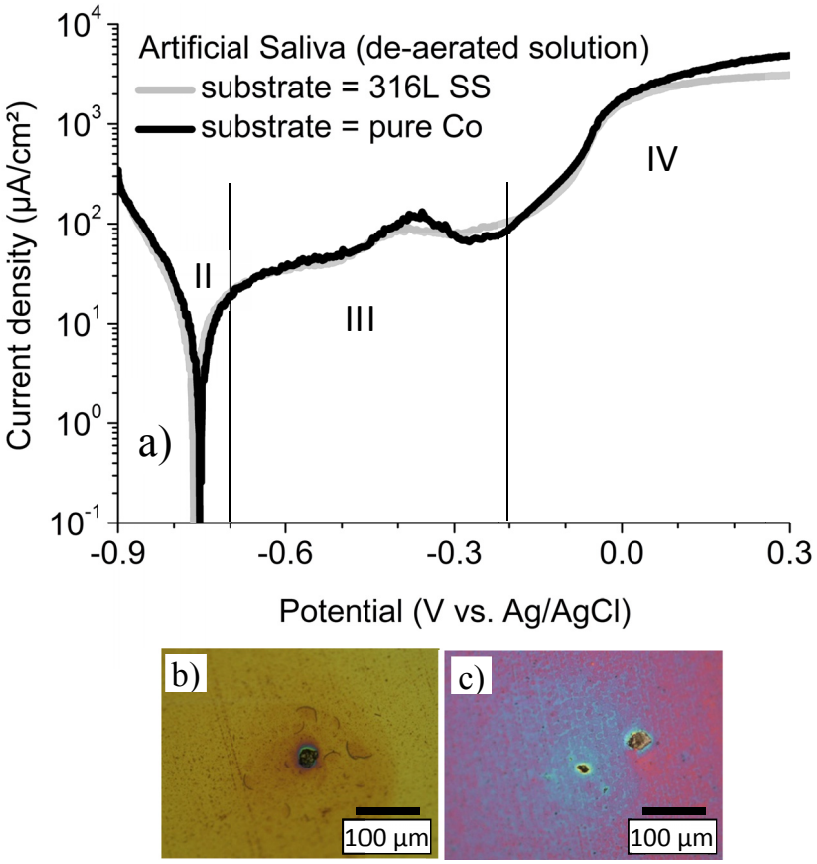

Fig. 4. Polarisation curves (1 mV/s) of the Co-Mo nanocrystalline coatings in artificial saliva (de-aerated solution). Optical images of the surface after polarisation curves: (b) 316L SS and (c) pure Co

General corrosion was observed in the Ringer's solution whereas pitting corrosion was found in artificial saliva. Therefore, the corrosion resistance of these coatings may be improved by adding inhibitors and/or compressive stresses. This will be the goal of the future studies.

Acknowledgments

This work was supported by the bilateral programme PHC POLONIUM (project #35214UK). The French Embassy in Poland and the Ministry of Foreign Affairs (France) are warmly acknowledged for providing a cotutelle PhD grant to M.L.

REFERENCES

[1] A.A. Karimpoor, U. Erb, K.T. Aust, G. Palumbo, Scripta Mater. **49** (7), 651-656 (2003).

[2] P. Cavaliere, Int. J. Fatigue **31** (10) 1476-1489 (2009).

[3] L.P. Bicelli, B. Bozzini, C. Mele, L. D'Urzo, Int. J. Electrochem. Sci. **3** (4), 356-408 (2008).

[4] Y.M. Wang, S. Cheng, Q.M. Wei, E. Ma, T.G. Nieh, A. Hamza, Scripta Mater. **51** (11) ,1023-1028 (2004).

[5] L. Wang, Y. Gao, T. Xu, Q. Xue, Mater. Chem. Phys. **99** (1), 96-103 (2006).

[6] D.H. Jeong, F. Gonzalez, G. Palumbo, K.T. Aust, U. Erb, Scripta Mater. **44** (3), 493-499 (2001).

[7] M.C. Roco, C.A. Mirkin, M.C. Hersam, WTEC Panel Report on 'Nanotechnology Research Directions for Societal Needs in 2020: Retrospective and Outlook', Chapter 11, pp. 361-388, September 2010, Springer Editions.

[8] V.Q. Kinh, E. Chassaing, M. Saurat, Electrodepos. Surface Treat. **3** (3), 205-212 (1975).

[9] V.S. Kublanovskii, Y.S. Yapontseva, Y.N. Troshchenkov, V.A. Gromova, Russ. J. Appl. Chem. **83** (3), 440-444 (2010).

[10] L. Anicai, S. Costovici, A. Cojocaru, A. Manea, T. Visan, Trans. IMF **93** (6), 302-312 (2015).

[11] H. Krawiec, V. Vignal, M. Latkiewicz, Mater. Chem. Phys. **183**, 121-130 (2016).

[12] K.S. Raja, D.A. Jones, Corros. Sci. **48** (7), 1623-1638 (2006).